RESEARCH ARTICLE
doi: 10.2306/scienceasia1513-1874.2009.35.261

ScienceAsia 35 (2009): **261–267**

Phase transition behaviour and dielectric properties of $Na_{0.5}K_{0.5}NbO_3$-$LiTaO_3$-$LiSbO_3$ lead-free piezoceramic

Pornsuda Bomlai[a,c,*], **Supasarote Muensit**[b,c], **Steven J. Milne**[d]

[a] Materials Science Program, Faculty of Science, Prince of Songkla University, Songkhla 90112, Thailand
[b] Department of Physics, Faculty of Science, Prince of Songkla University, Songkhla 90112, Thailand
[c] NANOTEC Centre of Excellence at Prince of Songkla University, Songkhla 90112, Thailand
[d] Institute for Materials Research, University of Leeds, Leeds LS2 9JT, UK

[*]Corresponding author, e-mail: ppornsuda@yahoo.com

Received 22 May 2009
Accepted 27 Aug 2009

ABSTRACT: Lead-free piezoelectric ceramics have attracted considerable attention as new piezoelectric materials for replacing $Pb(Zr,Ti)O_3$ (PZT)-based ceramics because of environmental protection reasons. Among lead-free piezoelectric systems, the ternary system of $Na_{0.5}K_{0.5}NbO_3$-$LiTaO_3$-$LiSbO_3$ has proven to be an outstanding lead-free piezoceramic with properties almost comparable to undoped PZT. In this study, addition of $LiSbO_3$ to the $0.95\,Na_{0.5}K_{0.5}NbO_3$-$0.05\,LiTaO_3$ lead-free piezoceramic composition showed a change from an orthorhombic to a tetragonal crystal system in samples prepared by reaction-sintering. The limit of solid solution along the compositional join, $(0.95-x)Na_{0.5}K_{0.5}NbO_3$-$0.05\,LiTaO_3$-$x\,LiSbO_3$, occurred at $x \sim 0.06$. Differential scanning calorimetry analysis and measurements of dielectric constant as a function of temperature indicated broad Curie peaks from which it was inferred that the samples were not chemically homogeneous. Curie temperatures decreased from ~425 °C for $x = 0$, to ~345 °C for the limiting $x = 0.06$ composition. Improvement of dielectric properties was obtained for $LiSbO_3$ modified samples. Microstructures exhibited secondary recrystallization, with $LiSbO_3$ addition giving rise to a small reduction in average grain size.

KEYWORDS: solid-solution, DSC analysis, reaction sintering, Curie temperature measurement

INTRODUCTION

Lead oxide-based piezoelectric ceramics such as lead zirconate titanate ($Pb(Zr,Ti)O_3$, PZT) are widely used for piezoelectric actuators, sensors, and transducers due to their excellent piezoelectric properties[1–3]. It is believed that their high piezoelectric response is related to the morphotropic phase boundary (MPB) between rhombohedral and tetragonal phases[4,5]. However, the toxicity of lead oxide and its high vapour pressure during processing has led to a demand for alternative piezoelectric materials.

Ceramics based on sodium potassium niobate ($(Na_{0.5}K_{0.5})NbO_3$, NKN) were considered as promising candidates due to attractive piezoelectric properties and Curie temperature. However, it is very difficult to obtain dense and well-sintered NKN ceramics by an ordinary sintering process. New solid solutions of NKN with other ABO_3-type compounds, e.g., $LiTaO_3$, $LiSbO_3$, and special fabrication techniques, e.g., spark plasma sintering have been used to improve sintering behaviour and electrical properties[6–10]. Among them, the mixed alkali niobate-tantalates solid solution system $[Na_{0.5}K_{0.5}NbO_3]_{1-x}$-$[LiTaO_3]_x$ (NKN-LT) has been reported to exhibit a polymorphic phase boundary (PPB) between orthorhombic and tetragonal phase-fields near room temperature at $0.05 < x < 0.06$[11]. Unlike that of the PZT system, this crystal structure transition from orthorhombic to tetragonal symmetry with doping is not due to the MPB in the NKN-LT system but compositionally shifting polymorphic phase transitions downward to near or at room temperature[12–14]. The PPB is quite similar to the frequently used MPB to enable phase coexistence but the crystal structure of the compositions near a PPB seems more sensitive to temperature. Compositions close to the PPB give the highest values of d_{33} piezoelectric charge coefficients (the induced charge per unit force applied in the same direction) in the system, reaching a value of ~200 pC/N at $x = 0.05$ with a corresponding Curie temperature (T_c) of ~420 °C. Saito et al[15] studied a wider range of related solid solutions, corresponding to the general formula $(K_{0.5}Na_{0.5})_{1-x}Li_xNb_{1-y}Ta_yO_3$. The composition $x = 0.03$ and $y = 0.2$, close to the PPB of this system, gave $d_{33} = 230$ pC/N with a T_c of 323 °C.

The NKN-LT-$LiSbO_3$ composition was first syn-

thesized by Saito et al[16]. The reactive template grain growth method resulted in enhancement of piezoelectric properties, giving a high value of $d_{33} = 416$ pC/N for $\langle 001 \rangle$ grain-oriented ceramics. The improvement was attributed to the existence of a PPB and $\langle 001 \rangle$ orientation.

Although the highest piezoelectric coefficients were demonstrated for textured ceramics fabricated using reactive template grain growth, these fabrication procedures are rather complicated and would be costly for commercial production. Hence it is important to optimize properties in conventional, randomly orientated ceramic samples. For example, Fu et al[17] have used conventional ceramic processing techniques to fabricate ceramics of the $(Na_{0.52}K_{0.44})(Nb_{0.96}Sb_{0.06})O_3$-0.04 $LiTaO_3$ system, and a high d_{33} of ∼335 pC/N was obtained.

In this study, $LiSbO_3$ was added to 0.95 NKN-0.05 LT. The base for achieving intrinsically enhanced properties is on the formation of a PPB between the orthorhombic and tetragonal phases. It is believed that more spontaneous polarization states are available owing to the coexistence of two kinds of ferroelectric phases. The PPB can be expected with changing the content of $LiSbO_3$. The phase transition behaviour and various dielectric properties of NKN-LT ceramics as a function of the $LiSbO_3$ content were investigated in detail. Ceramic samples were fabricated using a reaction-sintering method, which was employed because of the particularly high volatility of lithium and antimony oxides.

MATERIALS AND METHODS

Samples with a composition of $(0.95 - x)Na_{0.5}K_{0.5}NbO_3$-$0.05$ $LiTaO_3$-x $LiSbO_3$ were fabricated by the conventional mixed-oxide process using K_2CO_3, Ta_2O_5 (>99.0% purity, Aldrich), Na_2CO_3, Nb_2O_5 (99.9+% purity, Aldrich), Li_2CO_3 (>99.0% purity, Fluka), and Sb_2O_5 (99.995% purity, Aldrich) as starting powders. First, the $Na_{0.5}K_{0.5}NbO_3$ was prepared. The two carbonate powders are moisture-sensitive; thermogravimetric analysis indicates that dehydration is completed at ∼200 °C. In order to avoid compositional errors when weighing out the $Na_{0.5}K_{0.5}NbO_3$ precursor mixture, the starting reagents were dried in an oven for 24 h before use. Dried powders were cooled to room temperature and stored in the dessicator until immediately before weighing in the correct proportions. The starting materials were transferred to a 100 mm-diameter cylindrical plastic jar, partially filled with 10 mm-diameter alumina grinding balls. Sufficient ethanol was added to just cover the powder and grinding media. Ball-milling was carried out for 24 h, followed by drying at 120 °C, prior to grinding with an alumina mortar and pestle to break up large agglomerates formed during drying. The mixtures were calcined in alumina crucibles with loosely fitting lids at 800 °C for 2 h. For reaction sintering, the NKN powders were ground, weighed, and ball-milled again for 24 h with Ta_2O_5 and the volatile Li_2CO_3 and Sb_2O_5 components to obtain the compositions $(0.95 - x)Na_{0.5}K_{0.5}NbO_3$-$0.05$ $LiTaO_3$-x $LiSbO_3$ (NKN-LT-LS) for $x = 0.0$, 0.02, 0.04, 0.06, and 0.10. No second powder calcination stage was employed prior to sintering. The mixed powders were dried, ground, and pressed at 100 MPa into 1.5 cm diameter discs and sintered in air at temperatures of 1075 °C for 2 h in closed crucibles.

The polished ceramic samples were examined at room temperature using X-ray powder diffraction (XRD, Philips X′ Pert MPD, Ni-filtered CuK_α radiation) to identify the phase(s) formed. The microstructures of the as-sintered surfaces of the samples were imaged directly using scanning electron microscopy (SEM, Jeol JSM-5800LV). The average grain size was calculated by the mean linear intercept method. Differential scanning calorimetry (DSC7, PerkinElmer) was carried out in a N_2 atmosphere at a heating rate of 10 °C/min. To investigate dielectric properties, a silver electrode (Metech, Elverson, PA) was painted on both sides of the surfaces of the disc samples and fired at 600 °C for 10 min. The capacitance and dissipation factor (D) of the samples were measured as a function of temperature with a heating rate of 3 °C/min using a high precision LCR meter (LCR 821, Gw INSTEK) at 1 kHz from which the dielectric constant was calculated.

RESULTS AND DISCUSSION

XRD patterns of $(0.95 - x)Na_{0.5}K_{0.5}NbO_3$-$0.05$ $LiTaO_3$-x $LiSbO_3$ ceramics sintered at 1075 °C for compositions $x = 0$–0.1 are displayed in Fig. 1. Samples with $0 \leqslant x \leqslant 0.06$ showed a perovskite structure, indicating that Li^+ and Sb^{5+} had completely diffused into the NKN-LT lattice to form solid solutions. The intensity ratio of the pair of peaks at $2\theta = 45$–$46.5°$ in each pattern is used as an indication of the tetragonal/orthorhombic phase content[18]. The lower angle peak in the pair corresponds to the 022 peak of an orthorhombic NKN-LT phase, whereas it is the 002 peak for tetragonal NKN-LT[19,20]. The neighbouring higher angle peak is the orthorhombic 002 peak and the 200 peak of tetragonal NKN-LT. Hence the orthorhombic phase is the expected phase for the $x = 0$ composition, and $I_{022}/I_{002} \sim 1.7$.

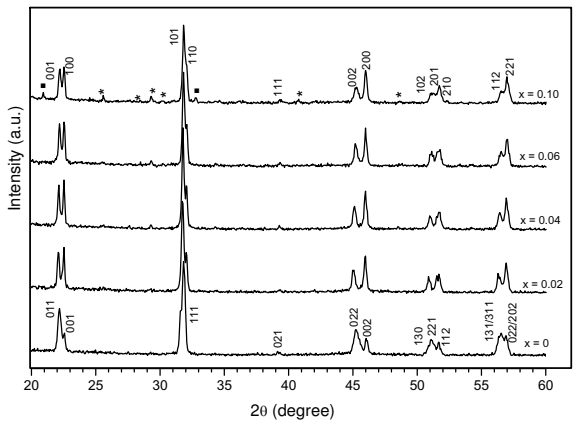

Fig. 1 XRD patterns of NKN-LT-LS samples sintered at 1075 °C for 2 h (* = $K_6Li_4Nb_{10}O_{30}$ [22]; ■ = $LiSbO_3$ [21]).

The phase boundary at room temperature between orthorhombic and tetragonal phases on the NKN-LT binary join occurs around 6 mol % LT[11]. However, the values of peak intensity ratio of all the Sb-modified samples were much lower, ∼0.5–0.8. This change suggests that the $LiSbO_3$ solid solutions are mainly tetragonal with some co-existing orthorhombic phase, thus giving intensity ratios slightly higher than expected for single-phase tetragonal samples[18].

Second-phase $LiSbO_3$ was detected in the $x = 0.1$ samples (Fig. 1). This indicated a limit of the LKN-LT-LS tetragonal solid solution at or around $x = 0.06$[21]. All samples showed faint XRD peaks due to a tungsten bronze phase which has also been reported for various compositions along the binary NKN-LT join[11,22]. Its proportion did not appear to change with $LiSbO_3$ content.

Ceramic microstructures were also studied. It can be seen that all samples were well densified, showing a significantly improved sinterability compared to pure NKN ceramics. However, all compositions with $x = 0.02$–0.1 showed secondary recrystallization (secondary grain growth)[23] after reaction-sintering at 1075 °C (Fig. 2). In the higher x samples there was a reduction in the fraction of secondary grains. Changes in secondary grain growth characteristics gave a small decrease in measured average grain size from ∼4 µm for $x = 0$ to ∼3.7 µm for $x = 0.06$. In other perovskites such as $BaTiO_3$, secondary grain growth is often associated with liquid phase formation. A similar mechanism leading to bimodal grain size distributions is probable in the NKN-LT-LS system.

The DSC heating curves of samples were measured to reveal the phase transition temperatures. Fig. 3 shows an endothermic peak for the $x = 0$ sample at a temperature of 425 °C. This temperature is consistent with the reported Curie temperature for the ferroelectric-paraelectric phase transition for binary NKN-LT compositions[11]. At $x = 0.02$ there was a much broader endotherm, the transition temperature decreased from 425 °C to 403 °C, and an overlapping, much more diffuse peak centred around 385 °C (onset

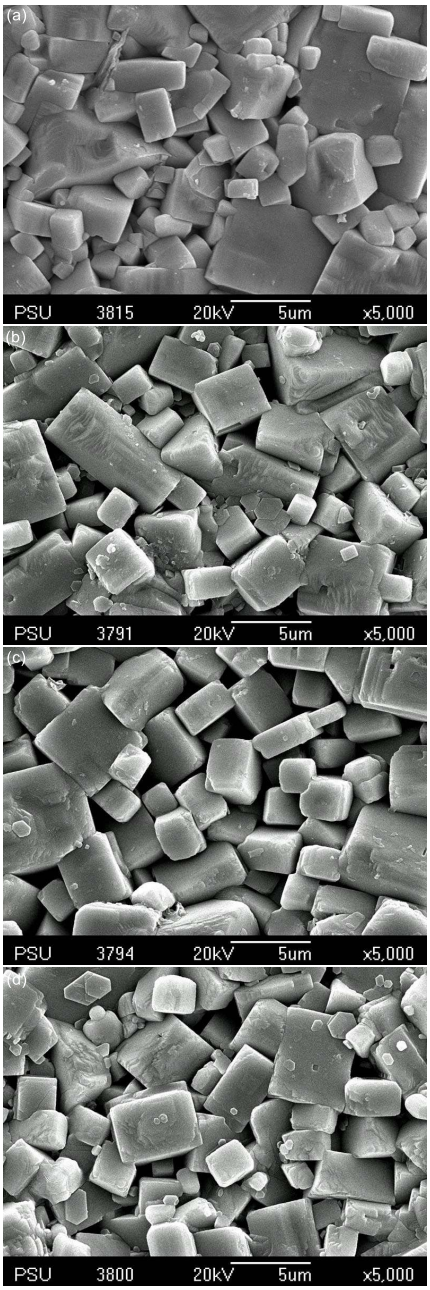

Fig. 2 SEM micrographs of $(0.95 - x)Na_{0.5}K_{0.5}NbO_3$-$0.05\,LiTaO_3$-$x\,LiSbO_3$ samples where x is: (a) 0 (b) 0.02 (c) 0.04 (d) 0.10.

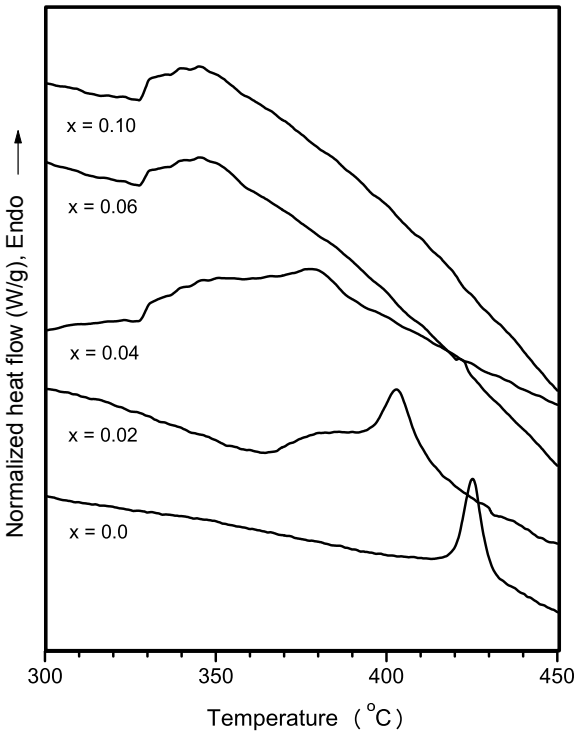

Fig. 3 DSC results of NKN-LT-LS samples.

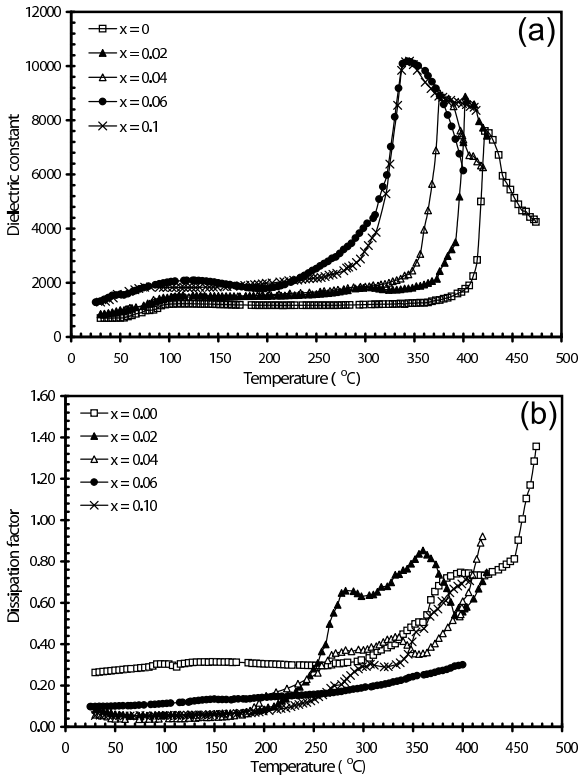

Fig. 4 Effect of NKN-LT-LS sample temperature on (a) dielectric constant (b) dissipation factor.

$\sim$365 °C) (Fig. 3). At $x = 0.04$ the DSC profile had similarities to the $x = 0.02$ sample, but the broader endotherm was more pronounced and occurred at a lower temperature ($\sim$360 °C, onset 340 °C) than for the $x = 0.02$ sample. A decrease in the temperature of the more distinct peak, from 403 °C to 378 °C, also occurred between the two compositions. For the $x = 0.06$ composition, only the broad endotherm was observed, centred at 346 °C (onset 328 °C). The DSC plot for $x = 0.1$ was very similar to $x = 0.06$, consistent with $x = 0.1$ lying beyond the limit of solid solution, $x \sim 0.06$. DSC peak temperatures are plotted in Fig. 5. However, the orthorhombic-tetragonal transition temperature from DSC analysis is difficult to determine exactly above room temperature.

The temperature dependence of the dielectric constant for comparable samples to those analysed by DSC is shown in Fig. 4. Dielectric Curie temperatures are also included in Fig. 5 to compare to DSC peak temperatures. The $x = 0$ Curie temperature of $\sim$422 °C from the dielectric data is similar to the DSC peak temperature (425 °C). A low-temperature discontinuity occurred in the dielectric plot at $\sim$55 °C (onset), consistent with transformation of the orthorhombic NKN-LT to the tetragonal phase. This low-temperature transition is evidence that the NKN-

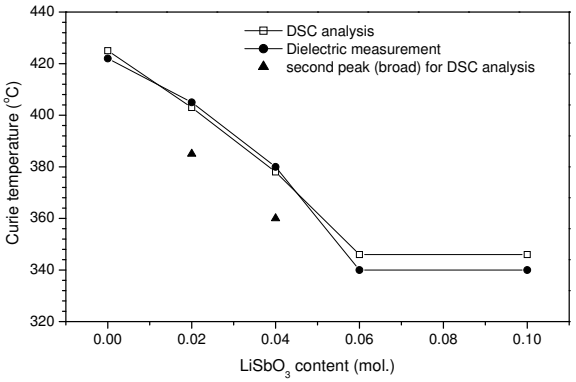

Fig. 5 Curie (peak) temperature from DSC analysis and dielectric constant measurement for NKN-LT-LS samples.

LT system does not possess a true morphotropic phase boundary. The orthorhombic to tetragonal transition occurs in $Na_{0.5}K_{0.5}NbO_3$ at $\sim$200 °C; the incorporation of $LiTaO_3$ progressively reduces the transition temperature until it reaches a value of $\sim$55 °C at NKN-5% $LiTaO_3$.

The dielectric data for the $x = 0.02$ samples again showed a Curie peak at temperatures consistent with

those inferred from the DSC data. For $x = 0.02$ the dielectric peak maximum occurred at ~405 °C but with a slight shoulder at 360–390 °C (Fig. 4a). The temperature range of the low temperature orthorhombic-tetragonal discontinuity for $x = 0.02$, 55–100 °C was similar to that for $x = 0$. The changes in XRD peak intensity ratios (Fig. 1) indicated that the $LiSbO_3$ solid solutions were composed mainly of a tetragonal phase; the dielectric anomaly at low-temperatures (Fig. 4a) presumably arises from the co-existing orthorhombic phase transforming to tetragonal phase on heating above 55 °C. The reasons for an additional faint irregularity at ~300 °C in the dielectric plot of $x = 0.02$ are uncertain (there was no evidence of a corresponding DSC effect). The $x = 0.04$ dielectric data showed a reduction in the dielectric constant peak temperature to ~380 °C; the peak was broader than for the $x = 0$ or $x = 0.02$ samples. The $x = 0.06$ sample continued the trend of decreasing Curie temperature and increased peak broadening; peak temperature was ~340 °C similar to the DSC value, 346 °C. The low-temperature region of the $x = 0.06$ dielectric plot displayed a weak broad dielectric peak, rather than a step increment as observed for $x = 0.0$–0.04 samples. The dielectric data for an $x = 0.1$ sample were similar to that for $x = 0.06$. The room temperature dielectric constant increased from ~690 in the $x = 0$ sample to ~1290 in the $x = 0.06$–0.10. Values of maximum peak dielectric constant increased from ~8000 in the $x = 0$ sample to ~10 000 in the $x = 0.06$–0.10 $LiSbO_3$ solid solution (Fig. 4a). The dissipation factor of modified samples reduced to ~0.05 at temperatures below 200 °C and reached a peak at near the T_c, after which it increased rapidly owing to conductive losses (Fig. 4b).

The trends in dielectric constant as a function of temperature are generally consistent with a ferroelectric material, and confirm that the DSC endotherms were due to ferroelectric–paraelectric transitions. For $x = 0.02$ and 0.04, the combined results suggest there are two different compositional ranges of solid-solution present in each sample. One of these may be closely related to the NKN-LT end-member, but with minor $LiSbO_3$ modification-giving rise to the distinct peak towards the higher temperature range of the DSC endotherm in $x = 0.02$ and 0.04. The second type of phase present in $x = 0.02$ and 0.04 may have higher levels of Li^+/Sb^{5+} substitution (giving lower Curie temperatures) and represent a more advanced stage of inter-diffusion reactions. Hence this phase more closely approaches the desired target solid solution formula, i.e., $(Na_{0.465}K_{0.465}Li_{0.07})(Nb_{0.93}Sb_{0.02}Ta_{0.05})O_3$ for $x = 0.02$. For $x = 0.06$, only the latter type of phase appears to be present. Compositional variations in each sample may contribute to the characteristic Curie peak profile above T_c, which was very different from that of a normal ferroelectric that follows the Curie-Weiss law.

The possible explanation for the phase heterogeneity inferred from the DSC and dielectric data is that samples have not reached chemical equilibrium after sintering for 2 h at 1075 °C. This seems to be particularly true for $x = 0.02$ and $x = 0.04$. The somewhat narrower temperature range of the DSC peak profile for the $x = 0.06$ sample is consistent with an improved reactivity during reaction sintering. Liquid formation during reaction sintering is plausible given the low melting point of the Sb_2O_5 component (380 °C), and the lack of full powder calcination prior to sintering. The formation of a narrower range of solid solution compositions in $x = 0.06$ than in $x < 0.6$ samples could be due to more liquid phase being formed in $x = 0.06$ samples during sintering. This would increase the rates of mass transport and inter-diffusion reactions, and hence increase component reactivity[18]. However, a degree of compositional heterogeneity persists in $x = 0.06$ samples, as Curie peaks are still relatively broad. Regions in the ceramic sample with slightly different compositions (ratios of constituent ions) would give rise to variations in Curie temperatures, with the net effect of producing a diffuse Curie peak.

The similarity in DSC and dielectric data for $x = 0.06$ and 0.1 samples indicate the limit of solid solution lies close to the $x = 0.06$ composition. The XRD data (Fig. 1) showed little evidence of peak broadening, but a previous study into phase development during conventional powder calcination of NKN-LT[18] indicated that d-spacings were insensitive to small changes in phase composition, and hence no noticeable XRD peak broadening would be observed.

Although the reaction sintering method adopted avoids powder calcination of lithium and antimony oxides, some volatilization losses may occur during sintering. Some of the differences in local composition may arise due to evaporation of volatile antimony and alkali-metal oxides, in addition to sluggish inter-diffusion reactions. Therefore, the surface may differ in composition from the interior of the pellet.

Severe phase inhomogeneity in binary NKN-LT ceramics made by conventional calcination of all powder components prior to sintering has been identified by others using SEM-EDX[24]. The inhomogeneity could not be eliminated by prolonged high-temperature annealing[24]. Therefore, problems

Table 1 Comparison of typical reported properties of NKN-LT-LS compositions.

Compositions	Density (g/cm^3)	ε_r	$\tan\delta$	T_c (°C)	Reference
$(K_{0.44}Na_{0.52}Li_{0.04})(Na_{0.84}Ta_{0.10}Sb_{0.06})O_3$	-	665	0.029	264	Ref. 26
$(Na_{0.52}K_{0.48-x})(Nb_{0.93-x}Sb_{0.07})O_3$-$x$ $LiTaO_3$ ($x = 0.0375$)	-	2165	-	271	Ref. 27
$(Na_{0.52}K_{0.48-x})(Nb_{1-x-y}Sb_y)O_3$-$x$ $LiTaO_3$ ($0 < x < 0.07$; $0 < y < 0.16$)	-	750–2500	-	230–430	Ref. 14
$(Na_{0.52}K_{0.48-x})(Nb_{0.96-x}Sb_{0.04})O_3$-$x$ $LiTaO_3$ ($x = 0.0375$–0.0575)	-	1644	-	340	Ref. 28
$(K_{0.44}Na_{0.52}Li_{0.04})(Na_{0.86}Ta_{0.10}Sb_{0.04})O_3$	4.51	1305	0.146	-	Ref. 29
$(K_{0.44}Na_{0.52}Li_{0.04})(Na_{0.80-x}Ta_{0.20}Sb_x)O_3$ ($x = 0$–0.04)	-	1258–1591	0.015–0.025	280–355	Ref. 30
$(1-x)K_{0.5}Na_{0.5}(Nb_{0.925}Ta_{0.075})O_3$-$x$ $LiSbO_3$ ($x = 0.035$)	-	~1200	~0.04	354	Ref. 31
$(0.95-x)Na_{0.5}K_{0.5}NbO_3$-0.05 $LiTaO_3$-x $LiSbO_3$ ($x = 0.02$–0.10)	4.32–4.44	849–1290	0.05–0.09	340–425	This work

in attaining compositional uniformity in NKN-LT-LS are not restricted to the reaction-sintering route employed. The refractory nature of Ta_2O_5 and Nb_2O_5 in conjunction with the volatility of the other oxide components makes this system very challenging in terms of ceramic fabrication.

Rubio-Marcos et al[25] reported that the formation of a solid solution between (Na,K)NbO_3-$LiTaO_3$-$LiSbO_3$ is extremely difficult to achieve due to the crystal structural differences between $KNbO_3$ and $NaNbO_3$, with perovskite crystal structures, and $LiTaO_3$ with a hexagonal pseudo-ilmenite crystal structure. However, several researchers have examined solid solution formation of related compositional series to the one presented here, involving different NKN-LT binary compositions and extending along the join to $LiSbO_3$ (Table 1)[14,26–31]; e.g., $(1-x)[(K_{0.5}Na_{0.5})(Nb_{0.925}Ta_{0.075})O_3]$-$x$ $LiSbO_3$ with x between 0 and 0.1, and also $(Na_{0.52}K_{0.48-x}Li_x)(Nb_{1-x-y}Sb_yTa_x)O_3$ ($0 < x < 0.07$, $0 < y < 0.16$)[14,31]. The results of conventional mixed oxide reactions for these compositions reveal that Li^+ and Sb^{5+} diffuse into the parent lattices to form a solid solution with a perovskite structure[31], but this seems to reduce its orthorhombicity because of the coexistence of orthorhombic and tetragonal phases[14]. Also, the T_c decreased gradually with increasing Sb content. For this work, it is reported to be an orthorhombic phase at $x = 0$ and tetragonal at $x \geqslant 0.02$. Therefore, coexistence of the orthorhombic and tetragonal phases is observed at $0 < x < 0.02$. Evidence for the alternative compositional join studied here also infers co-existence of orthorhombic and tetragonal phases at room-temperature. A comprehensive study of the NKN-LT-LS section of the phase diagram would be required to determine the full extent of the compositional area of solid solution formation in this region, and to confirm the extent to which tetragonal/orthorhombic phase-content is due to difficulties in achieving compositional equilibrium.

CONCLUSIONS

Lead-free piezoelectric ceramics prepared by reaction sintering of pre-calcined powders of $Na_{0.5}K_{0.5}NbO_3$ with Li_2CO_3, Ta_2O_5 and Sb_2O_5, according to the formula $(0.95-x)Na_{0.5}K_{0.5}NbO_3$-0.05 $LiTaO_3$-x $LiSbO_3$ displayed a change from orthorhombic to tetragonal crystal structure and broad Curie peaks inferring that the samples were not chemically homogeneous. Chemical modification of the end-member 0.95 $Na_{0.5}K_{0.5}NbO_3$-0.05 $LiTaO_3$ by $LiSbO_3$ reduced the Curie temperature from ~425 °C to ~345 °C for a composition $x = 0.06$, which lies close to the estimated limit of the $(0.95-x)Na_{0.5}K_{0.5}NbO_3$-0.05 $LiTaO_3$-x $LiSbO_3$ solid solution. Microstructures showed secondary grain growth; a slight decrease in grain-size with increasing $LiSbO_3$ modification was observed. The increment of dielectric properties was obtained for $LiSbO_3$ modified-samples. The room temperature dielectric constant increased from ~690 in the $x = 0$ sample to ~1290 in the $x = 0.06$–0.10 $LiSbO_3$ solid solution. Due to the good dielectric properties and sintering behaviour, the studied ceramics have a potential as a candidate for the application to lead-free piezoelectric ceramics.

Acknowledgements: This work was financially supported by Thailand Research Fund and Commission on Higher Education. The project was partly sponsored by NANOTEC Centre of Excellence at Prince of Songkla University, Thailand.

REFERENCES

1. Heartling GH (1999) Ferroelectric Ceramics: History and Technology. *J Am Ceram Soc* **82**, 797–818.
2. Uchino K (2000) *Ferroelectric Devices*, Marcel Dekker, New York.
3. Khaenamkaew P, Bdikin IK, Kholkin AL, Muensit S (2008) Local piezoresponse and ferroelectric domain of sol-gel $Pb(Zr_xTi_{1-x})O_3$ film. *Songklanakarin J Sci Tech* **30**, 59–63.
4. Zhang S, Xia R, Shrout TR (2007) Lead-free piezoelectric ceramics vs. PZT? *J Electroceram* **19**, 251–7.
5. Jaffe B, Cook W, Jaffe H (1971) *Piezoelectric Ceramics*, Academic, New York.
6. Zuo R, Rödel J, Chen R, Li L (2006) Sintering and electrical properties of lead-free $Na_{0.5}K_{0.5}NbO_3$ piezoelectric ceramics. *J Am Ceram Soc* **89**, 2010–5.
7. Hollenstein E, Davis M, Damjanovic D, Setter N (2005) Piezoelectric properties of Li- and Ta- modified $(K_{0.5}Na_{0.5})NbO_3$ ceramics. *Appl Phys Lett* **87**, 182905.
8. Li JF, Wang K, Zhang BP, Zhang LM (2006) Ferroelectric and piezoelectric properties of fine-grained $Na_{0.5}K_{0.5}NbO_3$ lead-free piezoelectric ceramics prepared by spark plasma sintering. *J Am Ceram Soc* **89**, 706–9.
9. Zhang BP, Li JF, Wang K, Zhang H (2006) Compositional dependence of piezoelectric properties in $Na_xK_{1-x}NbO_3$ lead-free ceramics prepared by spark plasma sintering. *J Am Ceram Soc* **89**, 1605–9.
10. Zang GZ, Wang JF, Chen HC, Su WB, Wang CM, Qi P, Ming BQ, Du J, Zheng LM, Zhang S, Shrout TR (2006) Perovskite $(Na_{0.5}K_{0.5})_{1-x}(LiSb)_xNb_{1-x}O_3$ lead-free piezoceramics. *Appl Phys Lett* **88**, 212908.
11. Guo Y, Kakimoto K, Ohsato H (2005) $(Na_{0.5}K_{0.5})NbO_3$-$LiTaO_3$ lead-free piezoelectric ceramics. *Mater Lett* **59**, 241–4.
12. Zhang S, Xia R, Shrout TR, Zang G, Wang J (2006) Piezoelectric properties in perovskite $0.948(K_{0.5}Na_{0.5})NbO_3$-$0.052LiSbO_3$ lead-free ceramics. *J Appl Phys* **100**, 104108.
13. Skidmore TA, Comyn TP, Milne SJ (2009) Temperature stability of $([Na_{0.5}K_{0.5}NbO_3]_{0.93}$- $[LiTaO_3]_{0.07})$ lead-free piezoelectric ceramics. *Appl Phys Lett* **94**, 222902.
14. Zuo R, Fu J, Lv D (2009) Phase transformation and tunable piezoelectric properties of lead-free $(Na_{0.52}K_{0.48-x}Li_x)(Nb_{1-x-y}Sb_yTa_x)O_3$ system. *J Am Ceram Soc* **92**, 283–5.
15. Saito Y, Takao H (2006) High performance lead-free piezoelectric ceramics in the (K,Na)NbO_3-$LiTaO_3$ solid solution system. *Ferroelectrics* **338**, 17–32.
16. Saito Y, Takao H, Tani I, Nonoyama T, Takatori K, Homma T, Nagaya T, Nakamura M (2004) Lead-free piezoceramics. *Nature* **432**, 84–7.
17. Fu J, Zuo R, Fang X, Liu K (2009) Lead-free ceramics based on alkaline niobate tantalite antimonate with excellent dielectric and piezoelectric properties. *Mater Res Bull* **44**, 1188–90.
18. Skidmore TA, Milne SJ (2007) Phase development during mixed-oxide processing of a $[Na_{0.5}K_{0.5}NbO_3]1-x$-$[LiTaO_3]_x$ powder. *J Mater Res* **22**, 2265–72.
19. ICDD (2001) Powder Diffraction File No. 32-0822, International Centre for Diffraction Data, Newton Square, PA.
20. ICDD (2001) Powder Diffraction File No. 71-0945, International Centre for Diffraction Data, Newton Square, PA.
21. ICDD (2001) Powder Diffraction File No. 84-2003, International Centre for Diffraction Data, Newton Square, PA.
22. ICDD (2001) Powder Diffraction File No. 48-0997, International Centre for Diffraction Data, Newton Square, PA.
23. Bomlai P, Sinsap P, Muensit S, Milne SJ (2008) Effect of MnO on the phase development, microstructures, and dielectric properties of $0.95Na_{0.5}K_{0.5}NbO_3$-$0.05LiTaO_3$ ceramics. *J Am Ceram Soc* **91**, 624–7.
24. Wang Y, Damjanovic D, Klein N, Hollenstein E, Setter N (2007) Compositional inhomogeneity in Li- and Ta-modified (K, Na)NbO_3 ceramics. *J Am Ceram Soc* **90**, 3485–9.
25. Rubio-Marcos F, Ochoa P, Fernandez JF (2007) Sintering and properties of lead-free (K,Na,Li) $(Nb,Ta,Sb)O_3$ ceramics. *J Eur Ceram Soc* **27**, 4125–9.
26. Hagh NM, Jadidian B, Safari A (2007) Property-processing relationship in lead-free (K, Na, Li)NbO_3–solid solution system. *J Electroceram* **18**, 339–46.
27. Fu J, Zuo R, Wang X, Li L (2009) Polymorphic phase transition and enhanced piezoelectric properties of $LiTaO_3$–modified $(Na_{0.52}K_{0.48})(Nb_{0.93}Sb_{0.07})O_3$ lead-free ceramics. *J Phys D* **42**, 012006.
28. Fu J, Zuo R, Wu Y, Xu Z, Li L (2008) Phase transition and electrical properties of Li-and Ta- substituted $(Na_{0.52}K_{0.48})(Nb_{0.96}Sb_{0.04})O_3$ piezoelectric ceramics. *J Am Ceram Soc* **91**, 3771–3.
29. Mgbemere HE, Herber R-P, Schneider GA (2009) Effect of MnO_2 on the dielectric and piezoelectric properties of alkaline niobate based lead free piezoelectric ceramics. *J Eur Ceram Soc* **29**, 1729–33.
30. Chang Y, Yang Z, Xiong L, Liu Z, Wang Z (2008) Phase structure, microstructure, and electrical properties of Sb-modified (K, Na, Li)(Nb, Ta)O_3 piezoelectric ceramics. *J Am Ceram Soc* **91**, 2211–6.
31. Lin D, Kwok KW, Chan HLW (2007) Phase structures and electrical properties of $K_{0.5}Na_{0.5}(Nb_{0.925}Ta_{0.075})O_3$-$LiSbO_3$ lead-free piezoelectric ceramics. *J Phys D* **40**, 6060–5.